

Universal Merging Histories of Dark-Matter Haloes

Eyal Neistein^{1,2*}, Andrea V. Macciò³ & Avishai Dekel¹

¹ *Racah Institute of Physics, The Hebrew University, Jerusalem, Israel*

² *Max-Planck-Institut für Astrophysik, Karl-Schwarzschild-Str. 1, 85748 Garching, Germany*

³ *Max-Planck-Institut für Astronomie, Königstuhl 17, 69117 Heidelberg, Germany*

ABSTRACT

We study merger histories of dark-matter haloes within various cosmological models by running a set of N -body simulations. The simulated cases include the Wilkinson Microwave Anisotropy Probe (WMAP) 5th year results, as well as Einstein-de Sitter universe, with several different power-spectrum shapes. We identify the scaling laws which allow a universal description of merger-trees independently on cosmological parameters. This is done by expressing the conditional mass function (CMF) in scaled variables of mass and time, and relaxing few symmetry assumptions which are usually adopted by the excursion set formalism. The CMF is then approximated by a global fitting function which is accurate for a large range of parameters; including different halo masses, redshifts, and cosmological models. The fit is significantly more accurate than previous estimates. Other statistical properties such as merger-rates and main-progenitor histories are shown to follow the scaling laws provided by the CMF. We show that our global fit can be used to transform merger-trees extracted from a given N -body simulation into a different cosmology or mass resolution. This technique is promising as it conserves the non-markov features of trees and it might be extended easily for handling substructures. It offers a simple way to study the effect of cosmology, dark energy models, and mass resolution on galaxies or other astrophysical objects. As an alternative approach, we confirm that main-progenitor histories follow a lognormal distribution, as was found by Neistein & Dekel. This description is shown to be more natural in capturing the behaviour of trees with time and descendant mass. However, due to the high level of similarity between the different simulations we cannot formulate a universal law describing the parameters of the lognormal distribution.

Key words: cosmology: theory — dark matter — galaxies: haloes — galaxies: formation — gravitation

1 INTRODUCTION

The growth of dark-matter haloes through merging and accretion is the driving force for many astrophysical phenomena. Accurate theoretical prediction for halo growth is thus a fundamental ingredient in various fields of cosmology, including structure formation, galaxy assembly, black holes growth and quasars physics.

The conditional mass function (hereafter CMF) has been an important tool in quantifying the growth of haloes. It is defined as the average number of progenitors which will merge into a descendant halo at a later time. The CMF was first introduced theoretically by the Extended Press-Schechter formalism (hereafter EPS, Bond et al. 1991; Bower 1991; Lacey & Cole 1993). Recent theoretical predictions use a variation of EPS, where the ellipsoidal collapse model is adopted instead of spherical collapse (Sheth & Tormen 2002; Moreno et al. 2008; Zhang et al. 2008). In addition, an empirical fit to the CMF which is based on N -body simulation was presented by Cole et al. (2008).

Although excursion set theories based on the ellipsoidal collapse are successful in predicting the halo abundance (i.e. halo mass function, see below), it seems that they do not provide a CMF which is significantly closer to N -body simulations than the traditional EPS result. Most of the current estimates of the CMF show significant variations from the results of N -body simulations where the number of progenitors can differ up to a factor of 3, especially for massive progenitors. The only estimate which was proved to be more accurate is the empirical study of Cole et al. (2008), where deviations can occasionally reach 50%. Since this fit was calibrated against the Millennium simulation (Springel et al. 2005), there is a need to verify it for cosmological parameters which better fit the recent Wilkinson Microwave Anisotropy Probe (WMAP) 5th year data (e.g. Komatsu et al. 2009).

A major target of this paper is to provide a better empirical description of the CMF as measured from N -body simulations. We work out the possible scaling laws which can be applied to the CMF in order to capture its details over large range of cosmological models, halo mass and redshifts. The result is an accurate fitting function, which offers a significant improvement in accu-

* E-mail: eyal@mpa-garching.mpg.de

racy over previous studies. This empirical fit is useful for various applications. It can help us distinguish between different analytical models, and can guide us to new improved versions of them. Such a fit can be used for generating monte-carlo merger-trees, which will accurately reproduce the results of N -body simulations. The effect of cosmology, environment density and different dark energy models can be studied, relating these ingredients to haloes and galaxies (e.g. Macciò et al. 2008). We discuss below few additional applications in more details.

Much effort has been invested in recent years in quantifying the abundance of haloes of a given mass (i.e. the halo mass function). The analytical model of Sheth & Tormen (1999) offers a significant improvement over the previous classical estimate of Press & Schechter (1974). On the other hand, the ever-growing dynamical range of N -body simulations allows an accurate measurement of the mass function with a negligible sampling scatter or cosmic variance (e.g. Jenkins et al. 2001; Warren et al. 2006; Reed et al. 2007). However, deviations between the theory and simulations still exist. For example, Tinker et al. (2008) have shown that deviations can increase as a function of redshift, reaching few tens of percents at $z = 2.5$. An accurate knowledge of the CMF can predict how the halo mass function will change with redshift. The benefit in using the CMF is that it includes much more information than the halo mass function, and the statistical noise is still small enough.

We will discuss a new methodology for scaling a given set of merger-trees into a different cosmological model or mass resolution. Although this technique requires an existing database of merger-trees extracted from a given N -body simulation, it offers an easy transformation for merger-trees to different redshift, mass resolution or cosmology. There are various advantages for using this method over monte-carlo generated trees. It can bypass the issue of non-markov features of the trees which correlates adjacent time-steps (Sheth & Tormen 2004; Neistein & Dekel 2008a), and it may be extended to include substructures and halo locations. Such a method can be very useful for semi-analytical modeling of galaxy formation, black hole growth, and dwarf galaxies assembly.

The usual line of thought in quantifying merger-trees starts with the definition of the CMF. This is the basic prediction of the EPS formalism, and it includes substantial information on the trees statistics. Once the CMF is known, more detailed statistics can be examined, such as main-progenitor histories and merger-rates. However, Neistein & Dekel (2008a, hereafter ND08a) have shown that a different path of reasoning is possible. These authors quantified the main-progenitor histories first, and then showed that it allows a full construction of merger-trees. Moreover, it was shown that the main-progenitor statistics is very regular, and follows a log-normal distribution in an appropriate mass variable (S , the variance of the smoothed density field). In this study we test this methodology for the set of simulations used here, and show that it allows an accurate description of N -body simulations which is more simple than the standard CMF approach. However, additional data is needed in order to formulate this approach independently on the cosmological model.

It should be noted that the CMF does not include all the information needed for describing merger trees. There are in general many different subsets of trees that can accurately fit a given function. Nonetheless, we will show in this work that the scaling laws of the CMF can provide a good estimate for the full statistics of the merger-trees, including main-progenitor histories and merger-rates.

This paper is organized as follows. In §2 we describe the set of N -body simulations we use, and the way merger trees are

Table 1. A summary of the N -body simulations used in this work, all with flat cosmology and with a Hubble constant of 72 km/s/Mpc. Particle mass is in units of $h^{-1}M_{\odot}$, box size is in Mpc. Each simulation follows the evolution 350³ particles.

Name	Ω_m	σ_8	Particle mass	Box
wmap5	0.258	0.796	4.54×10^8	90
lcdm	0.258	0.915	4.54×10^8	90
scdm1	1.0	0.77	1.76×10^9	90
scdm2 ($n = -2$)	1.0	0.8	1.76×10^9	90

constructed. Section 3 is devoted to the conditional mass function where we study its scaling properties, and we provide an accurate fitting function. In §4 we discuss an alternative description, using main-progenitor histories. A simple prescription on how to scale a given simulation is developed in §5. We summarize the results and discuss them in §6. Additional statistical properties of merger-trees which are not critical for the body of the paper are added in Appendix A. Throughout the paper we use log to designate \log_{10} , natural logarithm is written as \ln .

2 THE SIMULATIONS

All simulations have been performed with PKDGRAV, a tree code written by Joachim Stadel and Thomas Quinn (Stadel 2001). The code uses spline kernel softening, for which the forces become completely Newtonian at 2 softening lengths. Individual time steps for each particle are chosen proportional to the square root of the softening length, ϵ , over the acceleration, a : $\Delta t_i = \eta \sqrt{\epsilon/a_i}$. Throughout, we set $\eta = 0.2$, and we keep the value of the softening length constant in co-moving coordinates during each run ($\epsilon=1.62 h^{-1}\text{kpc}$). Forces are computed using terms up to hexadecapole order and a node-opening angle θ which we change from 0.55 initially to 0.7 at $z = 2$. This allows a higher force accuracy when the mass distribution is nearly smooth and the relative force errors can be large. The initial conditions are generated with the GRAFIC2 package (Bertschinger 2001). The starting redshifts z_i are set to the time when the standard deviation of the smallest density fluctuations resolved within the simulation box reaches 0.2 (the smallest scale resolved within the initial conditions is defined as twice the intra-particle distance). For each simulation we stored more than 100 outputs from redshift 10 to redshift zero, in order to construct detailed merger trees. The parameters of the simulations used in this work are describe in Table 1.

In all simulations, dark matter haloes are identified using the FOF algorithm with linking length of 0.2 times the mean interparticle separation. Only haloes which include more than 20 particles are saved for further processing. For constructing merger trees, we started marking all the particles within the virial radius of a given haloes at $z = 0$ and we tracked them back to the previous output time. We then make a list of all haloes at that earlier output time containing marked particles, recording the number of marked particles contained in each one. In addition we record the number of particles that are not in any halo in the previous output time and we consider them as *smoothly* accreted.

We used the two criteria suggested in Wechsler et al. (2002) for halo 1 at one output time to be labeled a “progenitor” of halo 2 at the subsequent output time. In our language halo 2 will then be labeled as a “descendant” of halo 1 if i) more than 50% of the particles in halo 1 end up in halo 2 or if ii) more than 75% of halo

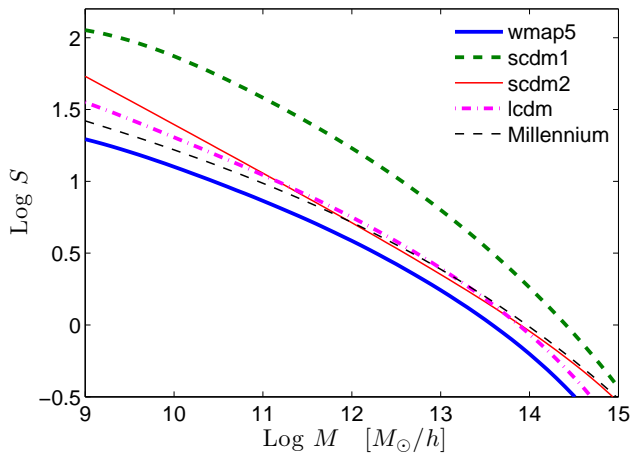


Figure 1. Various shapes of $S(M) = \sigma^2(M)$ for the set of simulations used in this work. $S(M)$ is defined as the variance of the initial density field, smoothed over spherical regions that include on average the mass M , and linearly extrapolated to $z = 0$. $S(M)$ is corrected according to the initial condition density field used for each simulation. As a reference we plot $S(M)$ that was used in the Millennium simulation (Springel et al. 2005).

1 particles that end up in any halo at time step 2, do end up in halo 2 (this second criterion is mainly relevant during major mergers). Thus a halo can have only one descendant but there is no limit to the number of progenitors.

We found evidence for the so-called ‘backsplash’ subhalo population (e.g. Knebe et al. 2008). These haloes have orbits that brought them inside the virial radius of their host at some earlier time, but without them been really accreted (i.e. they managed to come out from their host dark matter halo). We decided to treat them in two different ways according to their final fate: i) If after have been inside the main halo, the backsplash halo survives as isolated halo till the present time, than it is removed from the progenitor list of the parent halo (i.e. it is removed from the merger tree); ii) if the halo is accreted again (in a definite way) by the main halo at a later time step then it is considered as accreted the first time it entered the main halo. We found that back splash haloes are roughly 8% of the total progenitor number but they only marginally contribute (less than 2%) to the final halo mass.

According to the Extended Press-Schechter formalism the statistical properties of merger-trees are fixed by the density field at early times when perturbations grow linearly. All the statistical properties of this field are described by its variance, $S(M) = \sigma^2(M)$. Specifically, $S(M)$ is the variance of the density field, smoothed with a spherical top hat filter in space, and linearly extrapolated to $z = 0$ (for more details, see Lacey & Cole 1993). In fig. 1 we plot $S(M)$ for all the simulations used in this work. This comparison shows the predicted similarity between merger-trees of different simulations: we have two simulations with very similar $S(M)$ but different Ω_m (lcdm & scdm2). One simulation has a low value of σ_8 (wmap5), and the scdm1 simulation has a very different shape of $S(M)$.

In order to avoid deviations of $S(M)$ due to the small box size and cosmic variance we measured it directly from the initial condition density field used for each simulation. The values of σ_8 given in table 1 are those obtained by this calibration method. For the scale free simulation (scdm2) the box size is important as it limits

contributions from large scales to the field variance (see a detailed discussion in Smith et al. 2003). This effect bends $S(M)$ slightly at the high mass end, in agreement with the theoretical prediction.

3 CONDITIONAL MASS FUNCTION

This section is devoted to a comparison of the conditional mass function (CMF) as extracted from our set of N -body simulations. The scaling laws of the CMF are important as they highly constrain the behaviour of the full statistics of merger-trees. In Appendix A we show other statistical properties of trees, and demonstrate that they follow approximately the properties of the CMF found here.

According to the Extended Press-Schechter formalism (EPS, Bond et al. 1991; Bower 1991; Lacey & Cole 1993), the average number of progenitors in the mass interval $[M, M + dM]$, which will merge into a descendant halo M_0 after a timestep $\Delta\omega$, is given by

$$\frac{dN}{dM}(M|M_0, \Delta\omega)dM = \frac{M_0}{M} f(\Delta S, \Delta\omega) \left| \frac{dS}{dM} \right| dM. \quad (1)$$

Here $\omega \equiv \delta_c(z)/D(z)$, where $\delta_c(z) \simeq 1.68$ with a weak dependence on z , and $D(z)$ is the cosmological linear growth rate. $\Delta\omega \equiv \omega - \omega_0$ where the progenitors are identified at $\omega(z)$ and the descendant halo at ω_0 . We refer the reader to the appendix of ND08a for a detailed summary on how to compute ω , and a simple fitting function. The quantity $f dS$ describes the fraction of mass (out of the descendant halo) that is included within progenitors of mass in the range $[S, S + dS]$. According to EPS

$$f_{\text{ps}}(\Delta S, \Delta\omega) = \frac{1}{\sqrt{2\pi}} \frac{\Delta\omega}{(\Delta S)^{3/2}} \exp\left[-\frac{(\Delta\omega)^2}{2\Delta S}\right], \quad (2)$$

where $\Delta S \equiv S(M) - S(M_0)$, and f_{ps} is the specific solution of f given by the EPS formalism. In what follows we will use the name ‘CMF’ to designate dN/dM only.

In the language of the EPS formalism f_{ps} does not depend explicitly on the descendant halo mass M_0 or on the background cosmology. These parameters appear only in the transformation of ΔS and $\Delta\omega$ to mass and redshift. Even though the EPS formalism fails to produce accurate merger-trees (i.e. the *shape* of f_{ps} is not accurate), in general it might be that the universality of f_{ps} still exist. Sheth & Tormen (2002) and Cole et al. (2008) have tested the behaviour of f using N -body simulations, both showing non-negligible deviations from universality. However, these studies do not explore in detail the break in the universality, and do not test other models for f against N -body simulations. For example, Cole et al. (2008) have studied f only for descendant haloes identified at $z = 0$ and showed deviations of $\sim 50\%$ for various values of $\Delta\omega$ and halo masses.

The universality of f_{ps} is based on two ingredients: the dynamics of the spherical collapse model, and the properties of the initial density field when smoothed by a top-hat filter in k -space. Many works have investigated variations of this formalism by using the ellipsoidal collapse model, or smoothing filters with different shapes (Bond et al. 1991; Sheth & Tormen 2002; Zentner 2007; Desjacques 2008). Such models predict that f may depend on the descendant halo mass, breaking its simple universality. For example, Moreno et al. (2008) have stressed the fact that when using the ellipsoidal collapse model, f is universal if the variables $S(M)$ and $\Delta\omega$ are normalized by $S(M_0)$ and $\sqrt{S(M_0)}$ respectively. In its most general form f may depend on $S_0 \equiv S(M_0)$, ω_0 , and on the specific cosmology used. As will be shown below, neglecting the

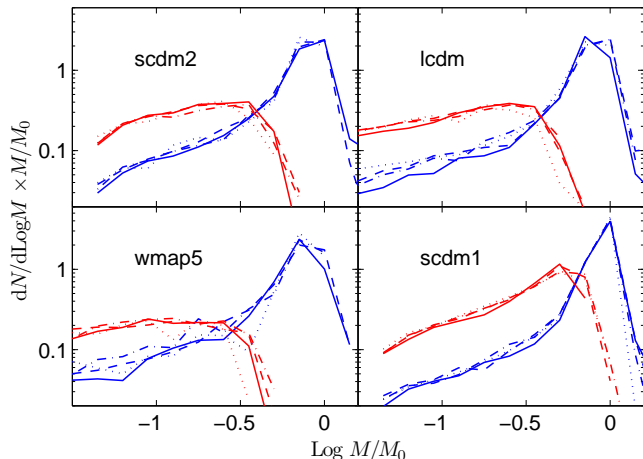


Figure 2. The self-similarity of the conditional mass function (CMF) with time. Each panel shows the CMF measured from one N -body simulation as indicated. The descendant halo is identified at $z_0 = 0, 1, 2, 3$ (solid, dashed, dotted-dashed, and dotted lines respectively), and the progenitors are identified at two lookback times $\Delta\omega = 0.5, 3$ (blue and red lines respectively). The distribution of the descendant masses at z_0 is selected such that it produces the same distribution of M_0 values at all z_0 , and $10^{12} \leq M_0 \leq 10^{13} h^{-1} M_\odot$. In the appendix we provide several other tests for the time self-similarity.

dependence on ω_0 and cosmology is possible, but the dependence on S_0 is essential for accurate description of the CMF.

3.1 Self-similarity in time

According to eq. 1 the CMF as predicted by EPS depends only on $\Delta\omega$ and not on the redshift z_0 where the descendant halo is defined. This self-similarity implies that merger-trees extracted at different redshifts are self-similar when using ω as the time variable. Indeed, ND08a and Genel et al. (2008) have verified this behaviour using merger-trees extracted from the large Millennium simulation (Springel et al. 2005). It was shown to work well for main-progenitor histories and merger-rates, with scatter of few percent up to $z \sim 5$ (see also Fakhouri & Ma 2008, who found deviations from this symmetry using a different definition of the halo mass).

In fig. 2 we show the level of self-similarity in time obtained by our four N -body simulations. The scdm1 & scdm2 simulations show small variations in the CMF between different z_0 , consistent with the sampling noise. The wmap5 and lcdm cosmologies show larger deviations, up to a factor of two for small progenitors, and for the time-step $\Delta\omega = 0.5$. However, the data do not show a monotonous trend with z_0 , hinting that our small statistics may contribute to the scatter. For example, the number of descendant haloes within a mass range $10^{12} \leq M_0 \leq 10^{13} h^{-1} M_\odot$ in the wmap5 cosmology is roughly (500,400,100,100) for $z_0 = (0, 1, 2, 3)$ respectively. It is also encouraging that better results were obtained for the Millennium simulation (as described above) and for large time-steps. Nonetheless, some deviation from self-symmetry may be related to the halo mass definition (i.e. the FOF linking length) and its evolution with redshift. As explained in section 2, we try to correct the merger-trees for ‘backsplash’ haloes. This correction may introduce some additional asymmetry between $z_0 = 0$ and higher redshifts.

The fact that merger-trees are similar when the descendant is

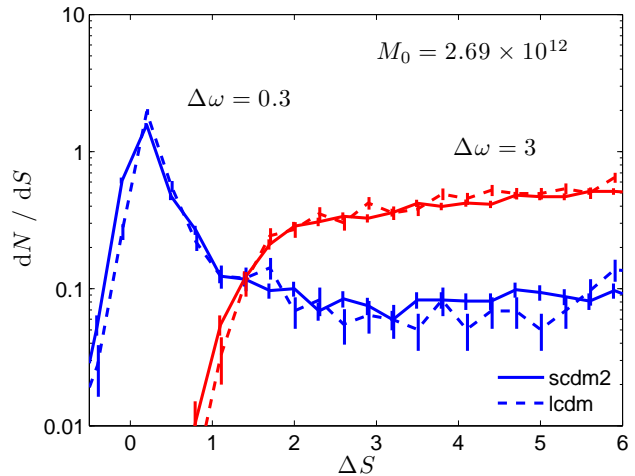


Figure 3. The self-similarity of the CMF for different expansion histories of the universe. The two sets of CMF are computed at $z_0 = 0$, for descendant mass in the range $10^{12} \leq M_0 \leq 10^{13} h^{-1} M_\odot$, and for $\Delta\omega = 0.3, 3$ (blue and red lines respectively). The solid (dashed) line shows results extracted from the scdm2 (lcdm) simulation. The distribution of the descendant masses at z_0 is matched in order to produce the same distribution of $S(M_0)$ values. The average descendant halo mass is indicated in units of $h^{-1} M_\odot$. Note that we plot the number of progenitors per unit of S , which is given by eq. 1 times $|dM/dS|$.

identified between $z = 0$ up to at least $z = 3$ is an important result. Due to the change in the effective cosmological parameters at large z (i.e. Ω_m, Ω_Λ), the merger trees at high- z correspond to a different cosmological model. Thus, the dependence of merger-trees on Ω_m, Ω_Λ and on the Hubble constant should be all folded into the time variable $\omega = \delta_c/D$. In fig. 3 we test this hypothesis by comparing the CMF from scdm2 and lcdm simulations. These simulations have a similar shape of $S(M)$ (see fig. 1) but very different Ω_m values. The agreement is within the Poisson sampling error-bars, proving that ω can scale properly different expansion histories of the Universe.

3.2 Different power-spectrum

Following the EPS formalism (eq. 2) the fraction of mass inside progenitors, $f_{ps}(\Delta S, \Delta\omega)$, depends only on $\Delta\omega$ and ΔS . As mentioned above, one could assume less universal form, $f(\Delta S, \Delta\omega|S_0)$ that will enable accurate description of the CMF in N -body simulations. In order to test this we plot f in fig. 4 for two sets of power-spectra. The results of the first comparison (left panels), between lcdm and wmap5 simulations, is very good, showing no significant deviation of f between the two models. This is obtained when the same values of M_0 are selected in each cosmology, or the same $S_0 = S(M_0)$. The difference between these two selection criteria is negligible, so we actually sample $f(\Delta S, \Delta\omega|S_0)$ for a small range in S_0 .

The second comparison (right panels), shown in fig. 4, is for wmap5 and scdm1 cosmologies. As seen in fig. 1 both $S(M)$ and its derivative dS/dM are very different between these two simulations. This is being translated into a large discrepancy in f when the same values of M_0 are chosen from both simulations. However, selecting a sample with the same S_0 values leaves f invariant, proving that $f = f(\Delta S, \Delta\omega|S_0)$ (at least for our limited set of data). For a given S_0 the values of M_0 in both simulations differ

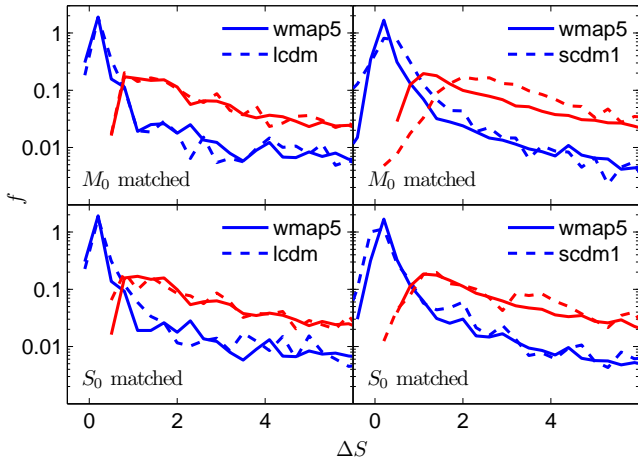


Figure 4. The fraction of mass within progenitors for different power-spectrum shapes and cosmologies. In each panel we compare results from two different simulations as indicated, with $\Delta\omega = 0.3, 2$, and descendant haloes which are selected at $z_0 = 0$. For the comparison between wmap5 & lcdm (left panels) we select haloes with $10^{13} \leq M_0 \leq 10^{14} h^{-1} M_\odot$ from wmap5 simulation. For the second comparison (right panels), the mass range of $10^{12} \leq M_0 \leq 10^{13} h^{-1} M_\odot$ in wmap5 was used. Selection of M_0 at the other cosmologies were chosen to match M_0 or S_0 distribution from wmap5, as indicated in each panel.

by a factor of ~ 10 , limiting the dynamical range for which we can check this f scaling.

The dependence of f on S_0 deserves a more careful test, probably with a larger set of N -body simulations, spanning a larger range of power-spectra. It is important to verify that such a dependence is not related to the *shape* of $S(M)$, as was found here. If this is true, it implies that a modification to the normalization of the power-spectrum (σ_8) which changes S_0 , will induce a non-trivial change to the CMF. Such a dependence on σ_8 is different from the simple scaling of the shape $\Delta\omega/\sqrt{\Delta S}$ that is used by EPS (see below).

3.3 Global fitting function

The EPS formalism suggests that the mass (ΔS) and time ($\Delta\omega$) variables can be scaled into a new variable $\nu \equiv \Delta\omega/\sqrt{\Delta S}$. In terms of ν , the function $f(\nu)\nu dS/d\nu$ should be universal. As shown above some dependence on S_0 is required, so we can try to use a function of the shape $f(\nu|S_0)$. This is tested in fig. 5 where we plot $f(\nu|S_0)$ for a fixed value of S_0 and for various $\Delta\omega$. The clear deviations from a unique line show that such a formulation is too simple and incompatible with the results of N -body simulations. This figure is very similar to the one given in Sheth & Tormen (2002) and Cole et al. (2008), and agrees with these previous results. Thus, we are forced to use a more general form $f = f(\Delta S, \Delta\omega|S_0)$.

We found that the fitting function below can fit the CMF from our set of N -body simulations for all time-steps larger than $\Delta\omega \sim 0.5$ and all S_0 values. We have looked for the simplest possible function that can fit the data, which is still similar to the EPS original function. The function we adopt is:

$$f(\Delta S, \Delta\omega|S_0) = a \frac{\Delta\omega}{\Delta S^{1.5}} \exp \left[-b \frac{\Delta\omega^2}{\Delta S} \right] + \quad (3)$$

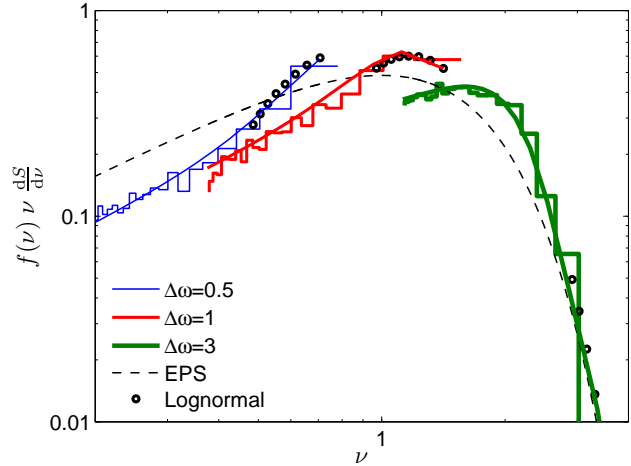


Figure 5. The limitation of using a fit of the shape $f(\nu|S_0)$. Simulation results are plotted as histograms, and are taken from the scdm2 simulation at $z_0 = 0$ with $\Delta\omega = 0.5, 1, 3$ and for average halo mass of $3 \times 10^{12} h^{-1} M_\odot$. The smoothed curves are derived from the global fit (eq. 3), EPS prediction is plotted as a thin dashed line, and the lognormal global fit to P_1 (eqs. 5 & 6) is plotted in circles (the latter is plotted only for $M > M_0/2$ where it should be identical to the CMF, see section 4).

$$c \frac{\Delta\omega^2}{\Delta S^3} \exp \left[-d \frac{\Delta\omega^{2.5}}{\Delta S^{2+\alpha}} \right],$$

where the parameters explicitly depend on S_0 in the following way:

$$\begin{aligned} a &= 0.215 + 0.0037 S_0 \\ b &= 0.414 + 0.0013 S_0^2 \\ c &= 0.0746 + 0.0382 S_0 \\ d &= 0.257 + 0.0568 S_0 \\ \alpha &= -0.0141 S_0 + 0.0056 S_0^2 \end{aligned} \quad (4)$$

In fig. 6 we compare our fitting function to the simulation data, showing that it accurately reproduces the trends found. The agreement between the fit and data is at the level of the statistical noise. The dependence on S_0 is mainly seen at low ΔS (corresponding to massive progenitors). We also show the EPS prediction and the fit derived by Cole et al. (2008), both independent on S_0 . Evidently, our fit agrees well with Cole et al. (2008) for intermediate and massive haloes. This is encouraging because the fits are based on different simulations and different merger-tree construction schemes. However, our fit breaks the symmetry of using only ν as was done by Cole et al. (2008), in this way it can capture the behaviour of the data for low mass haloes, and across various time-steps. The accuracy for different $\Delta\omega$ can be specifically seen in fig. 5.

The integral of f can be computed analytically only for $\alpha = 2$ ($S_0 \sim 2.5$), for the whole halo mass range we computed the integral numerically, yielding 0.75 up to 0.9, depending on the descendant mass and on the time-step. This predicts that a substantial fraction of the mass is not included in any progenitors but rather accreted from a ‘smooth’ component.

Throughout this work we mainly discuss the EPS formalism in its standard version. However, as mentioned in the introduction, versions of this formalism which use the ellipsoidal collapse model are presumably more accurate, as is indicated by their ability to predict accurate halo mass functions. We examine two such studies, the pioneer work of Sheth & Tormen (2002) and a more recent

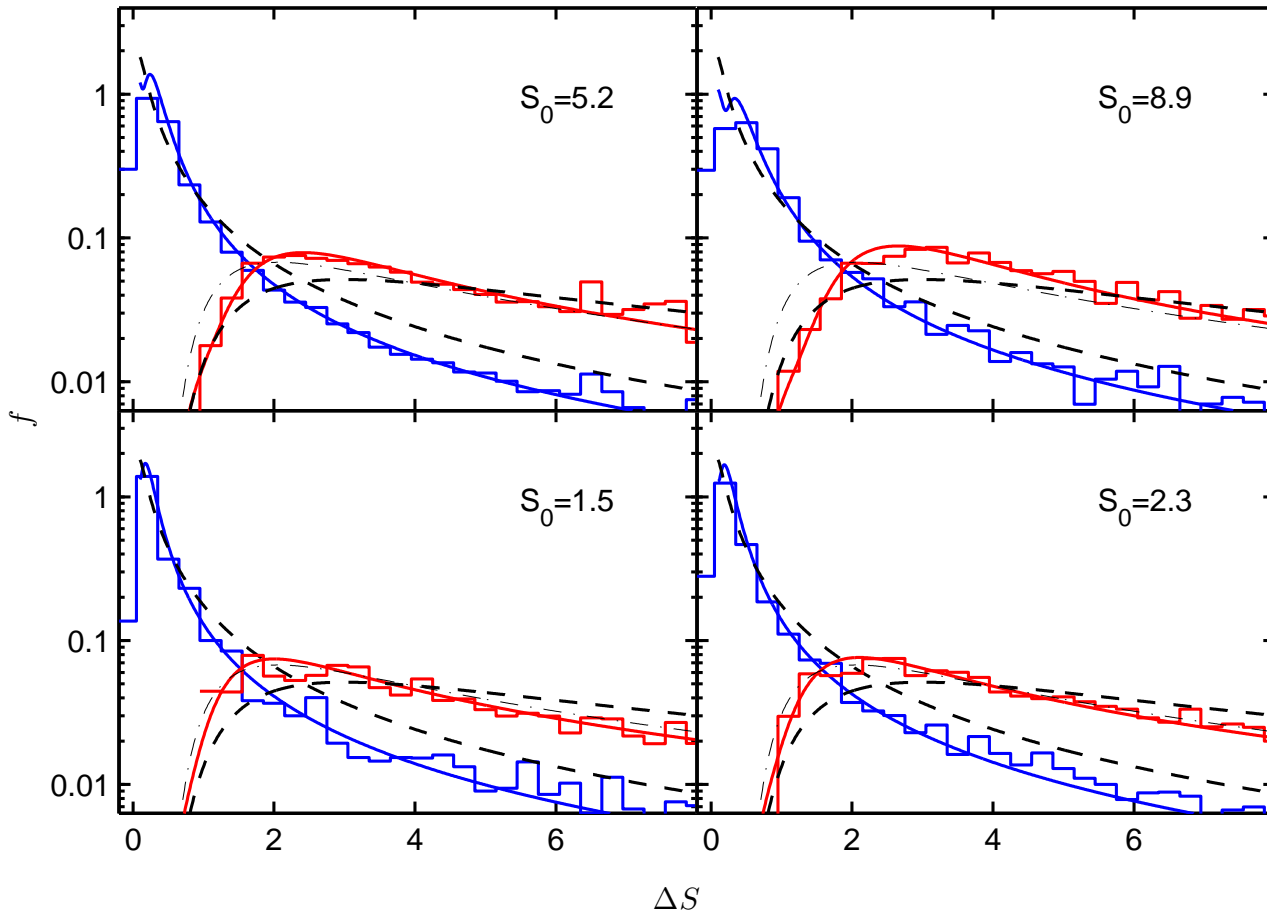


Figure 6. A global fit to $f(\Delta S, \Delta\omega|S_0)$ as defined in eqs. 3 & 4. Each panel shows the values of f for a given S_0 as indicated, and for time-steps of $\Delta\omega = 0.5$ & 3 (blue and red lines respectively). The simulation data were extracted and averaged from all the simulations used here, at $z_0 = 0$ & 1, using descendant mass with bin size of factor 3 in $h^{-1}M_\odot$. The histogram lines show results from simulations, smooth solid curves are plotted using our global fit, dashed lines are the EPS prediction, and the dashed-dotted lines are following the fit of Cole et al. (2008) (the latter are shown only for $\Delta\omega = 3$). Note that the EPS and Cole et al. (2008) are identical for all values of S_0 .

work by Moreno et al. (2008). Our interpretation of both studies is that the CMF as predicted by the spherical model is comparable in its accuracy to the one predicted by ellipsoidal collapse. This can be seen in figs. 7 & 8 of Sheth & Tormen (2002). More evidently, figs. 3-5 of Moreno et al. (2008) show that the spherical model gives better results for low mass descendant haloes, but this trend changes for massive haloes, where the ellipsoidal collapse is more accurate. A similar trend can be seen in fig. 6 here, where the deviations from EPS are shown to be larger for lower S_0 values.

4 MAIN-PROGENITOR HISTORIES

The “main-progenitor” history of a given merger-tree is constructed by following backward in time the most massive progenitor in each merger event. This is a useful definition as it allows us to follow a well defined branch of the tree. In addition, a quantitative description of the main-progenitor history highly constrains the full statistics of trees. Properties of main-progenitor histories were studied extensively, both analytically and using N -body simulations (Lacey & Cole 1993; Nusser & Sheth 1999; Firmani & Avila-Reese 2000; Wechsler et al. 2002; van den Bosch

2002; Neistein et al. 2006; Li et al. 2007; Neistein & Dekel 2008a; Zhao et al. 2008). Let us also mention that the main-progenitor is not always the most massive progenitor at a given time.

We define P_1 as the probability density to find a main-progenitor of mass $S(M_1)$ for a given descendant halo mass M_0 , and a time-step $\Delta\omega$. As was found by ND08a, P_1 can be well fitted by a lognormal distribution,

$$P_1(\Delta S_1|S_0, \Delta\omega) = \frac{1}{\sigma_p \Delta S_1 \sqrt{2\pi}} \exp \left[-\frac{(\ln \Delta S_1 - \mu_p)^2}{2\sigma_p^2} \right]. \quad (5)$$

Here $\Delta S_1 = S(M_1) - S(M_0)$, the parameters (σ_p, μ_p) depend on S_0 and $\Delta\omega$, and as usual $S_0 \equiv S(M_0)$. By definition, the integral over $P_1(\Delta S_1)$ equals unity for any S_0 and $\Delta\omega$.

Main-progenitor histories were constructed for all the simulations used in this work. Following ND08a, we confirm that the lognormal distribution fits accurately the simulation results. This was tested for all possible ranges of halo masses, redshift, and time-steps. As was mentioned by ND08a the fit becomes inaccurate for small time steps, typically for $\Delta\omega \lesssim 0.5$. Such a behaviour is found here as well. One exception to the above, where the lognormal fit is somewhat inaccurate, is for the scdm1 simulation at $z_0 = 0$. This may be due to the high sensitivity of ΔS in this cosmological

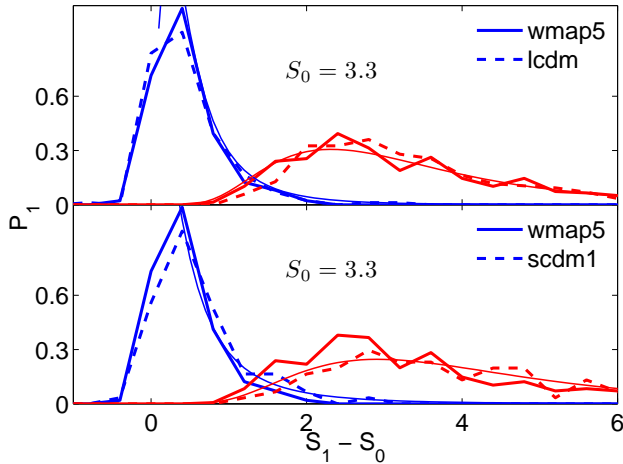


Figure 7. The full distribution of the main-progenitor in various cosmological models. Results are shown for descendant haloes defined at $z_0 = 1$, and main-progenitor selected at two time-steps, $\Delta\omega = 0.5, 3$. The descendant halo mass is in the range $10^{12} \leq M_0 \leq 4 \times 10^{12} h^{-1} M_\odot$ for wmap5 cosmology. M_0 in the other cosmologies were selected in order to match the same distribution in $S(M_0)$. Thin solid lines show the lognormal global fit, eq. 6, as computed for lcdm & scdm1 cases.

model (dS/dM is typically 7 times larger than other cases). The fact that the fit works well for $z \gtrsim 1$ data using the same cosmological simulation is encouraging. In fig. 7 we plot main-progenitor distributions for few cases of halo mass, z_0 and $\Delta\omega$, more examples can be found in Appendix B. The accuracy of the lognormal fit as plotted here is typical for the rest of the cases.

For each cosmology we are able to use a global fit, similar to the one suggested by ND08a¹. The fit approximates the standard deviation and average of $\ln \Delta S_1$ by

$$\begin{aligned} \sigma_p &= (a_1 \log S_0 + a_2) \log \Delta\omega + a_3 \log S_0 + a_4 \\ \mu_p &= (b_1 \log S_0 + b_2) \log \Delta\omega + b_3 \log S_0 + b_4. \end{aligned} \quad (6)$$

We provide numerical details for the values of these parameters in Appendix B. For a given S_0 , the evolution with time of σ_p and μ_p is simply linear in $\log \Delta\omega$. In fig. 5 we show that this evolution gives a very accurate fit to the relevant part of the CMF (the CMF and main-progenitor distribution are identical for $M > M_0/2$). We recall that such time-evolution was obtained for the CMF using much more complicated $\Delta\omega$ dependence (see eq. 3). Although both approaches discuss only the fitting possibilities, it seems that the main-progenitor gives a much simpler way to describe the merger history in an accurate way.

The simple behaviour of P_1 for each cosmology as seen in eq. 6 and in fig. 5 calls for a more global fit, which predicts the parameters of P_1 in other cosmological models. We compared P_1 for our set of simulations and found a high level of self-similarity, with the exception of the scdm1 case. Unfortunately we could not find a general law able to combine scdm1 with the other cosmological models. For example, choosing haloes with the same values of S_0 from scdm1 and other simulations does not yield the same results. To summarize, our study indicates that the main-progenitor

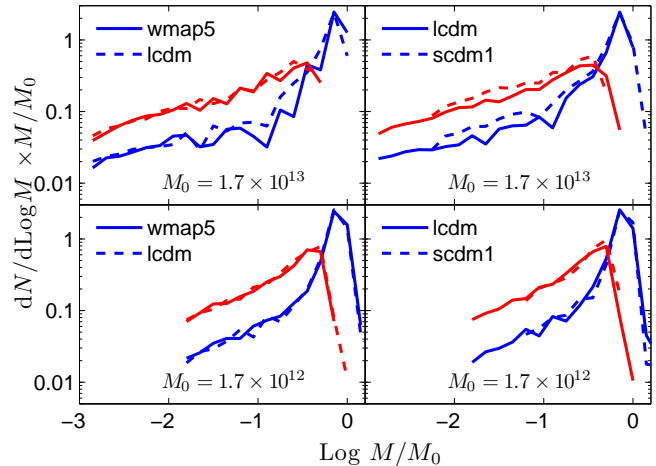


Figure 8. The conditional mass function, dN/dM , computed for different cosmological models using a transformation of the time-step $\Delta\omega$. In each panel we compare results from two different simulations and for the same descendant halo mass as indicated (mass is in units of $h^{-1} M_\odot$). The time-steps used for the lcdm cosmology are $\Delta\omega = 0.5, 2$. For the wmap5 (scdm1) cosmology we used time-steps which are different by a factor of 0.86 (1.8) in $\Delta\omega$. It seems that time transformation allows reasonable scaling of the merger-trees in these cases, although some deviations still exist.

distribution as extracted from N -body simulations has a universal lognormal shape. However, the dependence of the lognormal parameters on cosmology is not clear, and there is no theoretical explanation to this phenomena yet.

5 APPLICATIONS

An accurate fitting function for the CMF includes substantial information on halo growth, and it has various interesting applications: it can shed more light on the evolution of the halo mass function with redshift and cosmology (e.g. Tinker et al. 2008), it can constrain dark energy models, it is useful for generating monte-carlo merger-trees, and for predicting mass-accretion histories of the main-progenitor. Here we focus on a new methodology for re-scaling a given set of merger-trees between different cosmological models. We also discuss briefly the possibility of generating monte-carlo trees.

5.1 Re-scaling a given merger tree

There are many existing resources of N -body simulations and related merger-trees which are publicly available. The most useful one being the Millennium simulation (Springel et al. 2005) with its web-based database (Lemson et al. 2006). However, recent changes in the observed values of cosmological parameters (especially σ_8) make these simulations inaccurate for predicting observable quantities in our Universe. Here we suggest a new methodology to transform merger-trees into a different cosmological model, halo mass, and redshift. Such transformation can also be useful for enhancing the mass resolution of merger-trees. There are few benefits for this approach over the standard method of generating monte-carlo trees: (a) it can preserve the non-Markov behaviour of trees (see e.g. ND08a) (b) it might be easily extended to handle substructures

¹ Here we parameterize the fit according to S_0 , and not according to M_0 , as was done in ND08a, eq. 2

(c) it might be extended to accurate transformation of halo spatial locations.

We define case r as our reference data from a given merger-tree,

$$\{M_i | M_0, \Delta\omega, C\}_r \quad (7)$$

The data is defined as a set of progenitors M_i for a given descendant halo mass M_0 , time-step $\Delta\omega$ and a cosmological model C . Our target case is defined as a different cosmology \tilde{C} and descendant mass \tilde{M}_0

$$\{\tilde{M}_i | \tilde{M}_0, \tilde{\Delta\omega}, \tilde{C}\}_t \quad (8)$$

We are looking for a transformation of the kind

$$M_i \rightarrow \tilde{M}_i, \quad \Delta\omega \rightarrow \tilde{\Delta\omega} \quad (9)$$

that will yield a different set of progenitors, possibly for a different time-step, which will be consistent with the target case. We define the new transformed case as being consistent with the target case if the full statistical properties of the trees are similar. Specifically, we will require that the transformed progenitors will yield a CMF which is consistent with \tilde{M}_0 , $\tilde{\Delta\omega}$, and \tilde{C} . Note that our global fit was done for $f(\Delta S, \Delta\omega | S_0)$, as seen from eq. 1 the CMF includes two other components, the mass ratio M_0/M and the derivative dS/dM .

We start by searching for the most accurate transformation in $\Delta\omega$ which can compensate for the change in cosmology C , or descendant halo mass M_0 . This means we use only the transformation $\Delta\omega \rightarrow \tilde{\Delta\omega}$. In fig. 8 we plot the CMF for two sets of cosmologies, where $\Delta\omega$ is matched according to the global fit to the CMF. This time transformation is relatively accurate, although it can introduce large transformation in time (almost a factor of 2 in $\Delta\omega$ for one of the cases tested here). The original differences between the simulations can be seen in fig. 2 for reference. Although results are relatively accurate, it seems that the transformation in $\Delta\omega$ do not provide a uniform accuracy for all descendant masses. In fig. 9 we show how scaling $\Delta\omega$ can compensate for different descendant halo masses. This indicates that enhancement of mass resolution can be easily obtained. We emphasize that the $\Delta\omega$ transformations used here are obtained from matching the CMF, using our global fit (eq. 3).

This transformation in time is limited in few aspects: it is not always accurate, it can lower the time resolution of a merger-tree significantly, and it will stretch the non-markov correlations between consecutive time-steps in a way that might be different from the behaviour of the simulations. Our statistical sample do not allow to explore the last effect in detail, but we plan to pursue this in a future work.

A less trivial transformation is needed when the time scaling cannot provide an accurate enough solution. In this case we can transform the mass of the progenitor haloes in order to yield the same CMF. For any progenitor mass M we define \tilde{M} such that the integral over the number of progenitors will be invariant,

$$\tilde{M} : \int_{\tilde{M}}^{\tilde{M}_0} \left[\frac{dN}{dM} \right]_t dM = \int_M^{M_0} \left[\frac{dN}{dM} \right]_r dM. \quad (10)$$

This equation can be used to find the transformation $M \rightarrow \tilde{M}$ numerically using the global fitting function of eq.3. In fig. 10 we show that this transformation can yield perfect matching between very different CMF's. The only limitation in the accuracy is the goodness of our global fit, which is used to find the mass transformation above. As shown in fig. 10 the *same* mass transformation

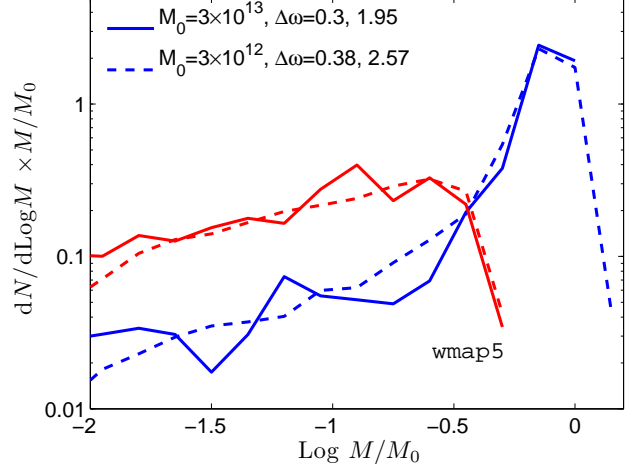


Figure 9. The conditional mass function (CMF) for different descendant halo masses, computed at different time-steps. We show that the transformation $\tilde{\Delta\omega} = 1.3 \times \Delta\omega$ can compensate accurately for changing the descendant mass M_0 .

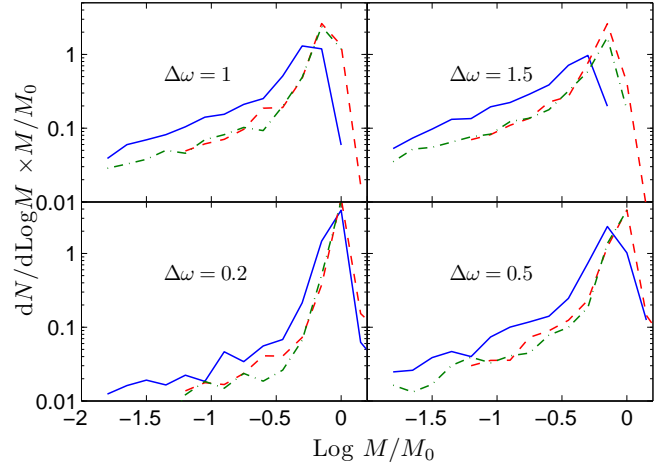


Figure 10. Scaling the mass in order to compensate for the change in dN/dM . We use eq. 10 to transform the mass of progenitors from wmap5 simulation (solid blue lines) into scdm1 (dashed red), both at the same time $\Delta\omega$. The mass transformation $M_i \rightarrow \tilde{M}_i$ was found according to the global fit at a *specific* time-step, $\Delta\omega = 1$. The same transformation is used to transform the actual progenitor masses for *all* time-steps used here. The dashed-dotted lines show the resulting histograms, which are similar to the target case. The descendant halo mass is $10^{12} h^{-1} M_\odot$.

is suitable for a large range of time-steps, so the deviations of the CMF fit at small time-steps do not degrade the accuracy of the mass transformation.

In general, one might use transformation of $\Delta\omega$ and mass according to the specific case needed. Time transformation are much more easy to perform, and should be preferred for cases where the resulting time resolution is not problematic. Mass transformation can be done as a second step, to increase the accuracy of the statistics by small variations in mass. For example, as tested above, using the results of the Millennium simulation (Springel et al. 2005) with a transformation $\tilde{\Delta\omega} = 0.86\Delta\omega$ should give merger-trees which

are consistent with the cosmological model WMAP5 for a large range of halo masses. For this simple case, the time transformation is consistent with the naive EPS prediction and scales like σ_8 .

5.2 Generating monte-carlo trees

Constructing monte-carlo merger-trees is doable once an accurate knowledge of the CMF is given for all time-steps. There are various algorithms that were applied to the EPS CMF, and can be easily generalized for other CMF's (Kauffmann & White 1993; Neistein & Dekel 2008b; Zhang et al. 2008). In this sense our fitting function for the CMF might be very useful for constructing monte-carlo trees that fit the results of N -body simulations. However, there are some limitations to this approach which we will emphasize here below.

As stated in the previous section, the quality of our global fit is poor for small time steps ($\Delta\omega < 0.5$). On the other hand, the time-step which is convenient for constructing monte-carlo trees is much smaller, around $\Delta\omega = 0.1$. Larger time-steps yield many progenitors in each merger event, and a large uncertainty in the predicted merging time of the haloes. As a result, we do not have an accurate fitting function for the CMF, which is appropriate for generating monte-carlo trees. More than that, an accurate fit for the CMF at small $\Delta\omega$ will not provide a solution, because the behaviour of merger-trees is highly non-markov at such small time-steps. This means that applying the CMF in consecutive time-steps without proper correlation between steps will generate large deviations in the merger histories (ND08a).

A possible solution to these problems is to look for a new CMF at small time-steps that will reproduce the CMF from N -body simulations at big time-steps. The CMF at small $\Delta\omega$ does not have to match N -body simulations, it can only be tested by applying it on few consecutive time-steps. Such a methodology was introduced by ND08a and found to produce good results. However, the resulting trees are fully markov, differing from N -body simulations. As a result of the above complications we think that this problem deserve more room than what is left here, and we postpone it to a future work.

6 SUMMARY AND DISCUSSION

In this work we study merger-histories of dark-matter haloes using a set of N -body simulations. The cosmological models simulated use $\Omega_m = 0.26$ & 1, along with various power-spectrum shapes. The main quantity we examine is the conditional mass function (CMF), and we verified the results with the statistics of main-progenitor histories and merger-rates.

It is first shown that merger-trees are self-similar in time when the variable $\omega = \delta_c/D$ is used ($\delta_c \sim 1.68$ and D is the cosmological linear growth rate). Such self-similarity was found before by Neistein & Dekel (2008a) and Genel et al. (2008) using the Millennium simulation (Springel et al. 2005), and it is verified here for different cosmological models. We prove that this symmetry also implies that ω can scale properly different expansion histories of the Universe.

For a given descendant mass and cosmology, the CMF depends on the lookback time in a way more complicated than the standard Extended Press-Schechter (EPS) prediction. This implies that the halo mass function should change in redshift in a different way than the linear $\sigma(M, z)$ behaviour. Indeed deviations of this kind were found recently by Tinker et al. (2008) using a large set

of N -body simulations. This demonstrates that studies of the CMF may constrain the halo mass function in a more detailed way.

We found that the CMF depends on the mass of the descendant halo, when written in terms of the field variance $\sigma^2(M)$. Using the above findings we derive a global fit to the CMF which is accurate for our set of simulations. We show that our fitting formula behaves better than EPS estimates based on the ellipsoidal collapse model (e.g. Sheth & Tormen 2002; Moreno et al. 2008), and also than other empirical fit (Cole et al. 2008). Our global fit shows deviation from the results of N -body simulations only at relatively small time-steps ($\Delta z < 0.5$). Recently, Zhao et al. (2008) studied the behaviour of main-progenitor histories for different cosmological models. They provide a fitting procedure for estimating median main-progenitor histories in any cosmological model. However, these authors used only *median* values, so the full CMF cannot be estimated from their results.

It was shown by Neistein & Dekel (2008a) that main-progenitor histories follow the lognormal distribution when plotted against $\sigma^2(M)$, this behaviour is also valid for our set of simulations. In this language the parameters of the distribution both depend linearly on $\log \Delta\omega$. Such a time-dependence is more simple than the dependence needed for an accurate CMF fit. Thus, the simple lognormal behaviour indicates that it might be useful to explore its origin further. We plan to do this in a future work.

We discuss one specific application of this study, which is to scale merger-trees given by an N -body simulation into a different cosmological model, mass range or redshift. We prove that these scalings yield merger-trees which are quite accurate, more than other approaches of constructing monte-carlo merger-trees. The scaling conserves the correlation of the progenitor masses between time-steps, an effect that would be hard to mimic in monte-carlo generated trees. There is still a need to study the scaling of substructures in a similar methodology. Substructures should be affected mostly by the mass ratio of the subhalo to its host halo, and by the dynamical time-scale within the host. Once these quantities are conserved, substructures might be easily scaled as well. This effect should be studied with high resolution simulations, and cannot be pursued here.

ACKNOWLEDGMENTS

We thank Raul Angulo, Mike Boylan-Kolchin, Ravi Sheth, and Simon White for useful discussions. We thank Andreas Faltenbacher for many helpful comments. Numerical simulations were performed on the PIA cluster of the Max-Planck-Institut für Astronomie and on the PanStarrs2 clusters at the Rechenzentrum in Garching. EN is supported by the Minerva fellowship. AM was partially supported by the Astrosim grant 2281. This research was supported by the German-Israeli-Foundation (GIF).

REFERENCES

- Bertschinger E., 2001, ApJS, 137, 1
- Bond J. R., Cole S., Efstathiou G., Kaiser N., 1991, ApJ, 379, 440
- Bower R. G., 1991, MNRAS, 248, 332
- Cole S., Helly J., Frenk C. S., Parkinson H., 2008, MNRAS, 383, 546
- Desjacques V., 2008, MNRAS, 388, 638
- Fakhouri O., Ma C.-P., 2008, MNRAS, 386, 577
- Firmani C., Avila-Reese V., 2000, MNRAS, 315, 457

- Genel S., Genzel R., Bouché N., Naab T., Sternberg A., 2008, ArXiv e-print 0812.3154
- Jenkins A., Frenk C. S., White S. D. M., Colberg J. M., Cole S., Evrard A. E., Couchman H. M. P., Yoshida N., 2001, MNRAS, 321, 372
- Kauffmann G., White S. D. M., 1993, MNRAS, 261, 921
- Knebe A., Arnold B., Power C., Gibson B. K., 2008, MNRAS, 386, 1029
- Komatsu E., et al., 2009, ApJS, 180, 330
- Lacey C., Cole S., 1993, MNRAS, 262, 627
- Lemson G., et al., 2006, ArXiv Astrophysics e-prints, astro-ph/0608019
- Li Y., Mo H. J., van den Bosch F. C., Lin W. P., 2007, MNRAS, 379, 689
- Macciò A. V., Dutton A. A., van den Bosch F. C., 2008, MNRAS, 391, 1940
- Moreno J., Giocoli C., Sheth R. K., 2008, MNRAS, 391, 1729
- Neistein E., Dekel A., 2008a, MNRAS, 383, 615 (ND08a)
- Neistein E., Dekel A., 2008b, MNRAS, 388, 1792
- Neistein E., van den Bosch F. C., Dekel A., 2006, MNRAS, 372, 933
- Nusser A., Sheth R. K., 1999, MNRAS, 303, 685
- Press W. H., Schechter P., 1974, ApJ, 187, 425
- Reed D. S., Bower R., Frenk C. S., Jenkins A., Theuns T., 2007, MNRAS, 374, 2
- Sheth R. K., Tormen G., 1999, MNRAS, 308, 119
- Sheth R. K., Tormen G., 2002, MNRAS, 329, 61
- Sheth R. K., Tormen G., 2004, MNRAS, 350, 1385
- Smith R. E., Peacock J. A., Jenkins A., White S. D. M., Frenk C. S., Pearce F. R., Thomas P. A., Efstathiou G., Couchman H. M. P., 2003, MNRAS, 341, 1311
- Springel V., White S. D. M., Jenkins A., Frenk C. S., Yoshida N., Gao L., Navarro J., Thacker R., Croton D., Helly J., Peacock J. A., Cole S., Thomas P., Couchman H., Evrard A., Colberg J., Pearce F., 2005, Nature, 435, 629
- Stadel J. G., 2001, PhD thesis, AA(UNIVERSITY OF WASHINGTON)
- Tinker J., Kravtsov A. V., Klypin A., Abazajian K., Warren M., Yepes G., Gottlöber S., Holz D. E., 2008, ApJ, 688, 709
- van den Bosch F. C., 2002, MNRAS, 331, 98
- Warren M. S., Abazajian K., Holz D. E., Teodoro L., 2006, ApJ, 646, 881
- Wechsler R. H., Bullock J. S., Primack J. R., Kravtsov A. V., Dekel A., 2002, ApJ, 568, 52
- Zentner A. R., 2007, International Journal of Modern Physics D, 16, 763
- Zhang J., Fakhouri O., Ma C.-P., 2008, MNRAS, 389, 1521
- Zhang J., Ma C.-P., Fakhouri O., 2008, astro-ph/0801.3459
- Zhao D. H., Jing Y. P., Mo H. J., Boerner G., 2008, ArXiv e-print 0811.0828

APPENDIX A: ADDITIONAL STATISTICS

A1 Self-similarity in time

In this section we provide more details on the accuracy of the self-similarity in time, as discussed in section 3.1. In fig. A1 we plot average main-progenitor histories for our set of simulations. The histories are plotted for descendant haloes identified at $z_0 = 0, 1, 2$. Comparing histories for different z_0 we see small deviations with

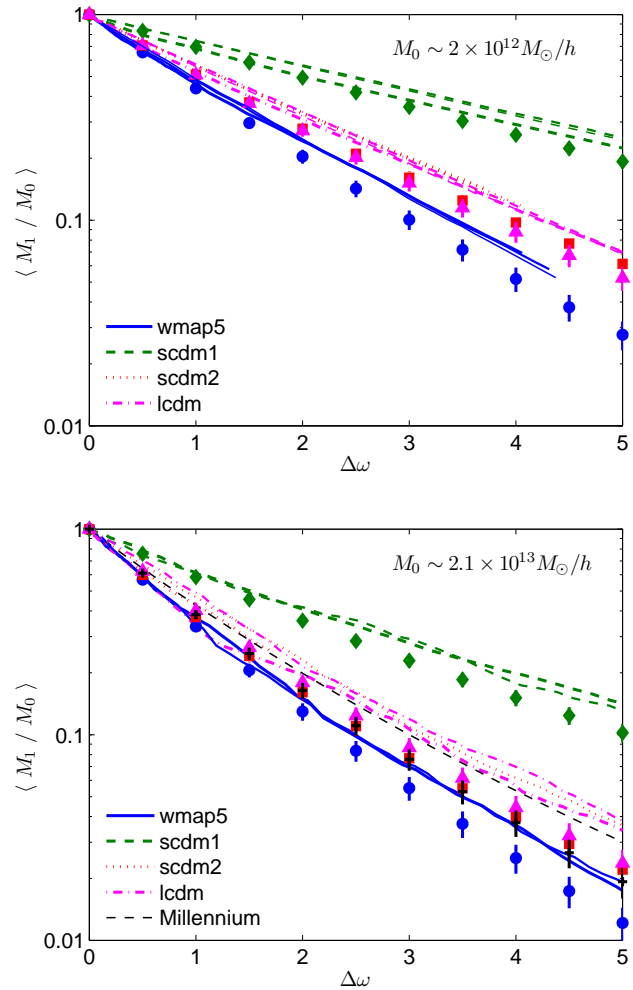


Figure A1. Average main-progenitor histories at different times. Smooth lines show main-progenitor histories for descendant halo M_0 identified at $z_0 = 0, 1, 2$ ($z_0 = 2$ was omitted for the high-mass bin due to a small statistical sample). Symbols and error-bars are the predictions of the EPS formalism following the formula of Neistein et al. (2006), and are independent on z_0 . The symbols shapes are diamonds, squares, triangles, circles and pluses for the scdm1, scdm2, lcdm, wmap5, and Millennium simulations respectively. It is evident that self-similarity in time is valid for all the simulations. The deviations of the EPS formalism with respect to N -body simulations are similar in all cases, although slight trends with cosmology and halo mass can be seen.

z_0 , reaching $\sim 20\%$ at $\Delta\omega = 5$ (for the scdm1 & lcdm simulations). It should be kept in mind that cosmic variance is non-negligible in this plot. We also plot the EPS prediction for the main-progenitor histories, as given by Neistein et al. (2006). The difference between the analytical EPS prediction and the results of N -body simulations seem to change slightly with halo mass. These results are sometimes different from the study of Zhao et al. (2008). We note that these authors compared *median* values from simulations against *average* values from the EPS formalism, as estimated by van den Bosch (2002). This makes their comparison less accurate than what is done here.

The full distribution of the main-progenitor, $P_1(\Delta S|S_0, \Delta\omega)$, is plotted in fig. A2 for descendant haloes selected at different z_0 .

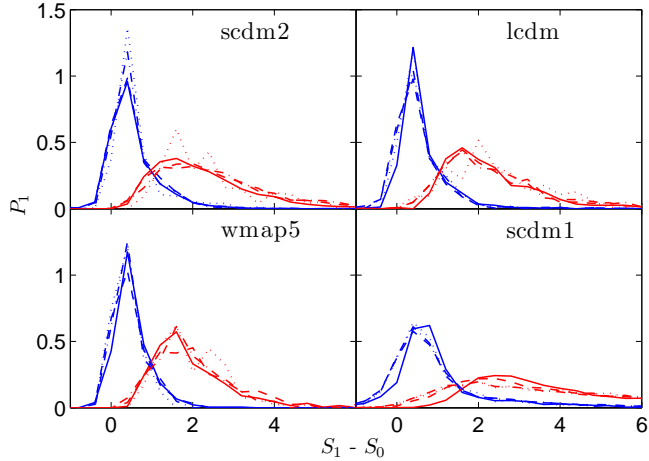


Figure A2. The full distribution of the main-progenitor mass at different times. In each panel we plot the results from one simulation as indicated, where the descendant halo mass M_0 is between 10^{12} and $10^{13} h^{-1} M_\odot$, and it is selected at $z_0 = 0, 1, 2, 3$ (solid, dashed, dashed-dotted, dotted lines respectively). Main-progenitors are followed backwards in time until $\Delta\omega = 0.5$ & 2 (blue and red curves respectively).

Here as well, self-similarity in time is shown to be accurate with the exception of the scdm1 simulation at $z_0 = 0$.

In figs. A3 & A4 we plot the mutual distribution of the two most massive progenitors. We show two dimensional histograms for descendant haloes selected at $z_0 = 0, 1, 2$. The results for scdm1 & scdm2 simulations show accurate similarity for different z_0 . However, the lcdm and wmap5 show deviations at the level of 10-20% in mass. These deviations decrease at larger time steps, so they might be connected to non-markov effects at small time-steps, and their variation with redshift. In addition, our treatment of ‘backsplash’ haloes may affect the results (see the discussion in section 3.1).

A2 Scaling merger trees

In this section we further examine the scaling of merger-trees as it was applied in section A2. We only show mutual distributions of the two most massive progenitors, (M_1, M_2) , as the main-progenitor distribution is highly constrained by the CMF (see e.g. Neistein et al. 2006). In fig. A5 we examine the time-transformation which was used to generate fig. 8. The results of the mass scaling as applied in fig. 10 are shown here in fig. A6.

APPENDIX B: A GLOBAL FIT TO THE MAIN-PROGENITOR DISTRIBUTION

In section 4 we claim that the lognormal distribution can be easily described for all time-steps and descendant masses using eqs. 5 & 6. This is shown in fig. B1, where full distributions of the main-progenitor mass are plotted. In tables B1 & B2 we summarize the parameters of the fits.

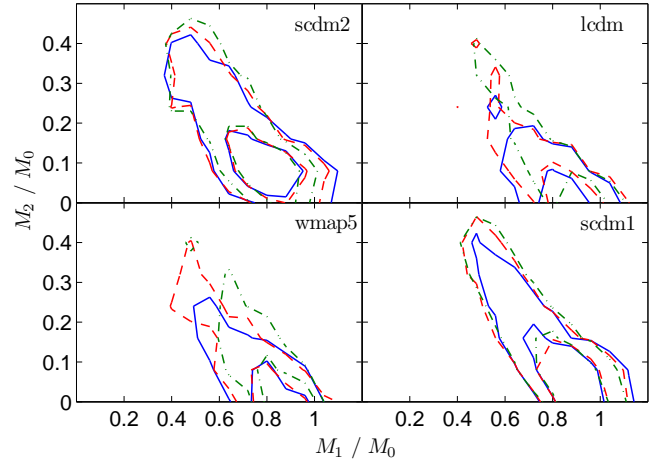


Figure A3. The mutual distribution of the two most massive progenitors (M_1, M_2) . Each panel shows results from one simulation as indicated. The descendant halo M_0 is identified at $z_0 = 0, 1, 2$ (plotted as solid, dashed, dashed-dotted lines respectively). The contour lines are plotted for 7 & 30% of the maximum histogram values. Descendant mass is between 10^{12} and $10^{13} h^{-1} M_\odot$, and $\Delta\omega = 0.3$ in all cases.

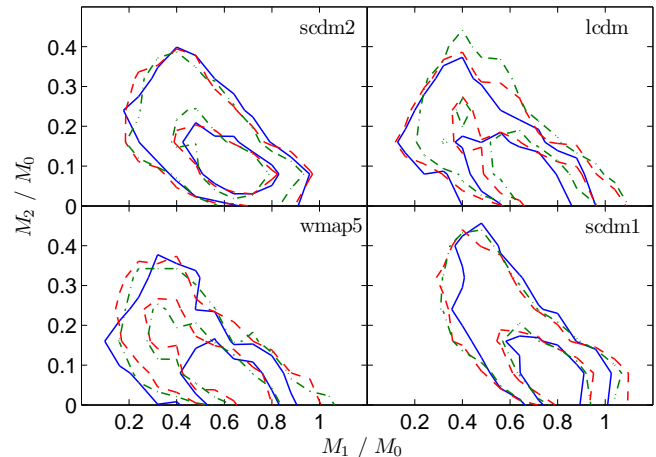


Figure A4. Same as fig. A3 but with $\Delta\omega = 0.8$.

Table B1. The coefficients used for the global lognormal fit, eqs. 5 & 6. The standard deviation of $\ln \Delta S$ obeys the equation $\sigma_p = (a_1 \log S_0 + a_2) \log \Delta\omega + a_3 \log S_0 + a_4$, where a_i are given below for each cosmology.

Simulation	a_1	a_2	a_3	a_4
wmap5	-0.333	-0.321	0.0807	0.622
scdm1	-0.0344	-0.608	0.185	0.697
scdm2	0.760	-1.085	0.184	0.668
lcdm	-1.209	0.205	0.245	0.571

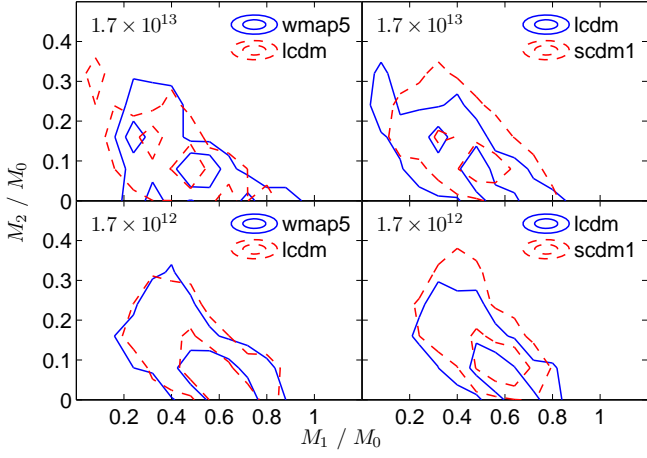


Figure A5. The mutual distribution of the two most massive progenitors (M_1, M_2), for $\Delta\omega$ matching. The same $\Delta\omega$ transformation is done as in fig. 8. The contour lines are plotted for 13 & 50% of the maximum histogram values. Descendant mass is indicated in units of $h^{-1}M_\odot$, $\Delta\omega = 1$.

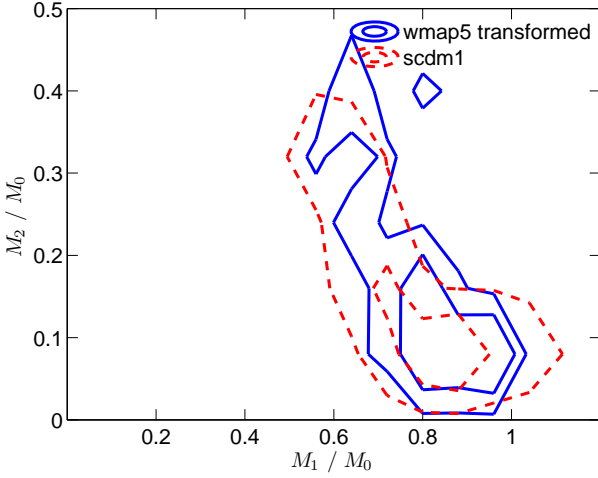


Figure A6. The mutual distribution of the two most massive progenitors (M_1, M_2), for mass matching. Mass transformation for wmap5 was done in the same way as in fig. 10. $\Delta\omega = 0.3$, $M_0 = 10^{12} h^{-1}M_\odot$.

Table B2. The coefficients used for the global lognormal fit, eqs. 5 & 6. The mean of $\ln \Delta S$ obeys the equation $\mu_p = (b_1 \log S_0 + b_2) \log \Delta\omega + b_3 \log S_0 + b_4$, where b_i are given below for each cosmology.

Simulation	b_1	b_2	b_3	b_4
wmap5	0.132	2.404	0.585	-0.436
scdm1	-0.8105	3.179	0.988	-0.513
scdm2	0.418	2.366	0.999	-0.647
lcdm	0.0788	2.418	0.671	-0.434

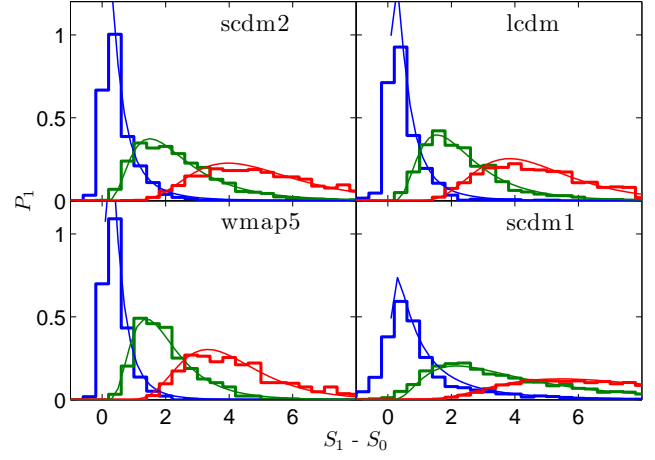


Figure B1. The full distribution of the main-progenitor for different cosmologies and time-steps. Descendant haloes are selected at $z_0 = 1$ with mass between 10^{12} and $10^{13} h^{-1}M_\odot$. Main-progenitor mass is followed backward in time until $\Delta\omega = 0.5, 2, 4$. Histograms show the simulation data, smooth lines are generated using our global fit.